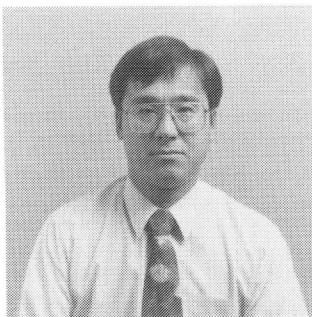
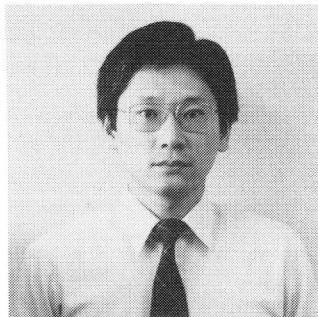


**STRAIN-SPACE PLASTICITY MODELING FOR COMPRESSIVE SOFTENING BEHAVIOR  
OF CONCRETE MATERIALS**

(Rearrangement of papers of Concrete Research and Technology, JCI, Vol.2, No.2, 1991 and J. Engrg. Mech., ASCE, Vol.118, No.8, 1992)



Eiji MIZUNO



Shigemitsu HATANAKA

**SYNOPSIS**

A strain-space-based plasticity model is proposed to represent the softening as well as hardening behavior of concrete under low confining pressure. A general strain-space formulation is presented in some detail by introducing the Lade type of loading function  $F$  and a new plastic potential function  $G$  defined in strain space. The incremental stress-strain relation is given in a tensorial form. Using the experimental data available from triaxial compression tests, the model parameters are determined, and model simulation is performed to demonstrate the model capability. It is confirmed that the proposed model can sufficiently predict the softening as well as hardening behavior of concrete materials under low confining pressure.

**Keywords:** concrete, constitutive law, plasticity theory, strain softening, strain space, stress space, stress-strain relation.

-----  
E. Mizuno is an associate professor of civil engineering at Nagoya University, Nagoya, Japan. He received his Doctor of Philosophy from Purdue University in 1981. His research interests include development of constitutive relations of engineering materials, such as steel, concrete, and soil, under cyclic loading. He is a member of JSCE and JCI.  
-----

-----  
S. Hatanaka is an associate professor of architectural engineering at Mie University, Tsu, Japan. He received his Doctor of Engineering Degree from Nagoya University in 1984. His research interests include experimental and analytical work on constitutive relations of concrete materials, such as plain and confined concrete, and normal- and high-strength concrete. He is a member of AIJ and JCI.  
-----

## 1. INTRODUCTION

It is well known that an increase in the toughness (energy absorption capacity) of concrete in the compressive zone of reinforced concrete (RC) members is quite effective for improving their ductility. An introduction of lateral confinement is considered one of the actual and effective ways to enhance the compression toughness of concrete. Although a use of the lateral reinforcing bars can introduce such lateral confinement, the magnitude of effective lateral pressure is not generally so high, e.g., less than 20 kgf/cm<sup>2</sup> (1.96 MPa) in compression. Therefore, the concrete, even with lateral reinforcing bars, causes the compressive softening behavior in a relatively higher strain region, which plays an important role in controlling the plastic deformation behavior of RC members.

Since experimental data for concrete in the compressive softening region have been lacking, there have been, so far, a few theoretical challenges for modeling a softening behavior of concrete [1][2][3][4][5]. To clarify such compressive softening behavior of concrete under low lateral confining pressure from the experimental point of view and to provide the experimental data for theoretical development of a concrete constitutive model, one of the writers has carried out a series of triaxial compression tests on concrete [6][7][8].

On the other hand, some other experimental studies have been reported on the complete stress-strain curves of concrete under triaxial compression [9][10][11]. In these reports, however, experimental data were obtained from specimens with height/diameter (H/D) ratio = 2 - 3. As has been pointed out by Van Mier [12] and Kosaka et al. [6], the uniaxial stress-strain curves obtained from specimens with different H/D ratios are quite different from each other, i.e., the softening portion of the stress-strain curve becomes steeper due to damage concentration as the H/D ratio increases. Kosaka et al. [6] have found that damage occurs in a relatively uniform manner inside a specimen with H/D = 1.

In the present study, therefore, by examining the experimental data of concrete specimens with H/D = 1 [6][7][8], a concrete constitutive model has been proposed to represent the strain-softening as well as strain-hardening behavior under low lateral confining pressure. The constitutive equation is formulated by using the strain-space-based plasticity theory, taking into consideration the representation capacity for the compressive softening behavior of concrete and the applicability to the finite element analysis of RC structures.

The Lade type of loading surface and the new plastic potential surface, in particular, are defined in the strain space, then employed into the strain-space-based constitutive equation. The material parameters incorporated in the proposed model are determined from triaxial compression test data including the softening part, and model simulations are performed to examine the model capability.

## 2. STRAIN-SPACE-BASED PLASTICITY FORMULATION

The stress-space plasticity formulation based on the Drucker's postulate [13] has been extensively employed for modeling strain-hardening behavior of engineering materials in general and concrete material in particular [14][15][16].

On the other hand, the strain-space plasticity formulation, which is basically derived from the Il'yushin's postulate [17], has been proposed to represent softening behavior as well as hardening behavior completely without a

mathematical discrepancy [3][18][19][20][21][22].

In the following, the strain-space-based plasticity formulation is briefly described.

## 2.1 Loading Function

A loading surface  $F$  defined in the strain space can be, in general, written as

$$F = F(\varepsilon_{ij}, \varepsilon_{ij}^p, f_p) = 0, \quad (1)$$

where  $\varepsilon_{ij}$ ,  $\varepsilon_{ij}^p$ , and  $f_p$  = strains, plastic strains, and a loading parameter that is related to a surface size and is usually a function of plastic work  $W_p$ , respectively.

If the shape of loading surface  $F$  in the strain space is assumed analogous to that of the well-defined loading surface  $f$  in the stress space, as pointed out by Naghdi and Trapp [18], the loading function  $F$  may be derived in the following manner: Assuming that an elastic behavior is linear and that the strains  $\varepsilon_{kl}$  can be decomposed into the elastic strains  $\varepsilon_{kl}^e$  and plastic strains  $\varepsilon_{kl}^p$ , the stresses  $\sigma_{ij}$  are given by the generalized Hooke's law as

$$\sigma_{ij} = C_{ijkl} \varepsilon_{kl}^e = C_{ijkl} (\varepsilon_{kl} - \varepsilon_{kl}^p), \quad (2)$$

where  $C_{ijkl}$  = the fourth-order elastic stiffness tensor. Substitution of stress tensor in Eq.(2) into the loading function  $f$  written in terms of stress variables yields the loading function  $F$  in terms of strain variables. For example, a use of isotropic hardening/softening type of loading surface,  $f = f(\sigma_{ij}, f_p)$ , leads to

$$\begin{aligned} f &= f(\sigma_{ij}, f_p) \\ &= f[C_{ijkl}(\varepsilon_{kl} - \varepsilon_{kl}^p), f_p] \equiv F(\varepsilon_{ij}, \varepsilon_{ij}^p, f_p) = 0. \end{aligned} \quad (3)$$

## 2.2 Loading Criteria

Some difficulties arise when the loading criteria corresponding to loading surface  $f$  are used in the stress-space formulation. For example, an explicit distinction cannot be made between strain softening and unloading conditions that are written as  $\partial f / \partial \sigma_{ij} d\sigma_{ij} < 0$ , nor between perfect plasticity loading and neutral loading conditions written as  $\partial f / \partial \sigma_{ij} d\sigma_{ij} = 0$ .

On the other hand, the loading criteria corresponding to loading surface  $F$  are mathematically expressed by

$$\frac{\partial F}{\partial \varepsilon_{ij}} d\varepsilon_{ij} > 0 \quad : \text{Loading (Hardening, softening, and perfect plasticity)} \quad (4.a)$$

$$\frac{\partial F}{\partial \varepsilon_{ij}} d\varepsilon_{ij} = 0 \quad : \text{Neutral loading} \quad (4.b)$$

$$\frac{\partial F}{\partial \varepsilon_{ij}} d\varepsilon_{ij} < 0 \quad : \text{Unloading.} \quad (4.c)$$

As can be understood from Eqs.(4a-4c), it becomes clear that the above loading criteria in the strain space do not result in such a contradiction

caused by loading criteria in the stress space. Thus, the strain-space-based plasticity may provide a useful approach to model the softening behavior of engineering materials such as soils, rocks, and concretes.

### 2.3 Flow Rule

According to the Il'yushin's postulate, the scalar product of the relaxation stress tensor  $\sigma_{ij}^p$  and the incremental strain tensor  $d\varepsilon_{ij}$  is always nonnegative on the loading surface  $F$  in the strain space. This condition is written mathematically as

$$\sigma_{ij}^p d\varepsilon_{ij} \geq 0, \quad (5)$$

where the relaxation stress  $\sigma_{ij}^p$  is defined as

$$\sigma_{ij}^p = C_{ijkl} d\varepsilon_{kl}^p. \quad (6)$$

The nonnegativeness of Eq.(5) guarantees the normality of the relaxation stress  $\sigma_{ij}^p$  to the loading surface  $F$ . In a similar manner to the derivation of the plastic strain increment  $d\varepsilon_{ij}^p$  in the stress-space formulation based on the Drucker's postulate, the relaxation stress  $\sigma_{ij}^p$  can be derived as

$$\sigma_{ij}^p = d\lambda \frac{\partial F}{\partial \varepsilon_{ij}}, \quad (7)$$

where  $d\lambda$  = a nonnegative scalar quantity; and  $\partial F / \partial \varepsilon_{ij}$  = the normal components to the loading surface  $F$ . Equation (7) corresponds to the associated flow rule defined in the stress-space formulation.

On the other hand, the introduction of plastic potential function  $G = G(\varepsilon_{ij}, \varepsilon_{ij}^p, f_p)$  leads to a nonassociated flow rule given by

$$\sigma_{ij}^p = d\lambda \frac{\partial G}{\partial \varepsilon_{ij}}. \quad (8)$$

The plastic strain increment  $d\varepsilon_{ij}^p$  can be written from Eq.(6) as

$$d\varepsilon_{ij}^p = [C_{ijkl}]^{-1} \sigma_{kl}^p = D_{ijkl} \sigma_{kl}^p. \quad (9)$$

where  $D_{ijkl}$  = a compliance tensor. Application of Eq.(8) into Eq.(9) leads to

$$d\varepsilon_{ij}^p = d\lambda D_{ijkl} \frac{\partial G}{\partial \varepsilon_{kl}}. \quad (10)$$

A similar derivation can be seen in the work by Han and Chen [3]. On the other hand, Klousis [22] showed a different form of flow rule that the vector of plastic strain increments is normal to the plastic potential function  $G$ .

### 2.4 Elastic-Plastic Constitutive Relations

A consistency condition of the loading function  $F = F(\varepsilon_{ij}, \varepsilon_{ij}^p, f_p)$  can be written as

$$dF = \frac{\partial F}{\partial \varepsilon_{ij}} d\varepsilon_{ij} + \frac{\partial F}{\partial \varepsilon_{ij}^p} d\varepsilon_{ij}^p + \frac{\partial F}{\partial f_p} df_p = 0, \quad (11)$$

where  $f_p$  = a function of the plastic work  $W_p$  whose incremental form  $dW_p$  is given

by  $\sigma_{ij} d\varepsilon_{ij}^p$ . Substituting the following relation:

$$df_p = \frac{df_p}{dW_p} dW_p = \frac{df_p}{dW_p} \sigma_{ij} d\varepsilon_{ij}^p \quad (12)$$

into Eq.(11), further substituting Eq.(10), and solving for  $d\lambda$  lead to

$$d\lambda = \frac{\frac{\partial F}{\partial \varepsilon_{ij}} d\varepsilon_{ij}}{-\frac{\partial F}{\partial \varepsilon_{ab}^p} D_{abcd} \frac{\partial G}{\partial \varepsilon_{cd}} - \frac{\partial F}{\partial f_p} \frac{df_p}{dW_p} \sigma_{ab} D_{abcd} \frac{\partial G}{\partial \varepsilon_{cd}}} \quad (13)$$

Backsubstitution of Eq.(13) into Eq.(10) and further application into the incremental linear elastic stress-strain relation  $d\sigma_{ij} = C_{ijkl}(d\varepsilon_{kl} - d\varepsilon_{kl}^p)$  yields the following incremental elastic-plastic constitutive relation in the strain space.

$$d\sigma_{ij} = \left[ C_{ijkl} - \frac{\frac{\partial G}{\partial \varepsilon_{ij}} \frac{\partial F}{\partial \varepsilon_{kl}}}{-\frac{\partial F}{\partial \varepsilon_{ab}^p} D_{abcd} \frac{\partial G}{\partial \varepsilon_{cd}} - \frac{\partial F}{\partial f_p} \frac{df_p}{dW_p} \sigma_{ab} D_{abcd} \frac{\partial G}{\partial \varepsilon_{cd}}} \right] d\varepsilon_{kl} \quad (14)$$

The comparison between the strain-space and stress-space formulations is presented in **Table 1**.

### 3. APPLICATION OF THE LADE LOADING FUNCTION

The research on softening behavior has been, so far, proceeded not only for concretes, but also for soils. Lade [23] proposed a stress-space-based plasticity model for strain softening as well as strain hardening of soils.

An analogous shape to that of the Lade loading surface defined in the stress space is here applied to those of the loading surface and plastic potential surface in the strain space. The loading function  $F$  and plastic potential function  $G$  will be derived in the following:

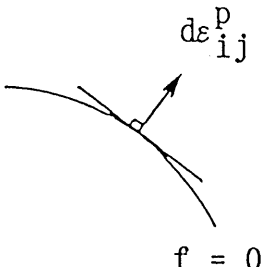
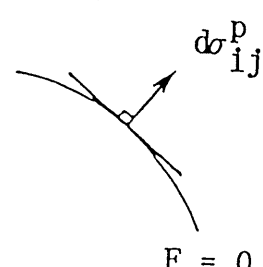
#### 3.1 Loading Function $F$

The Lade type of loading function  $f$  for material such as concrete with a tensile strength can be written in terms of stress invariants as [24]

$$f = (I_1 + a)^3 - [27 + f_p \left( \frac{P_a}{I_1 + a} \right)^m] \left[ \frac{1}{27} (I_1 + a)^3 - \frac{1}{3} (I_1 + a) J_2 + J_3 \right] = 0, \quad (15)$$

where  $I_1$ ,  $J_2$ , and  $J_3$  = the first invariant of stress tensor and the second and third invariants of the deviatoric stress tensors, respectively;  $P_a$  = the atmospheric pressure;  $m$  = the shape parameter;  $a$  = a magnitude of movement to the tensile direction along the hydrostatic pressure axis; and  $f_p$  = the loading parameter. The loading parameter  $f_p$  takes initially zero on the hydrostatic pressure axis, increases gradually up to the maximum value of  $\eta_1$  at a failure state, then decreases as the strain softening progresses.

Table 1. Comparison of Stress Space and Strain Space Formulations

Stress Space Formulation	Strain Space Formulation
(1)	(2)
(a) Loading Function	
$f = f(\sigma_{ij}, f_p) = 0$	$F = F(\varepsilon_{ij}, \varepsilon_{ij}^p, f_p) = 0$
(b) Loading Condition	
$\frac{\partial f}{\partial \sigma_{ij}} d\sigma_{ij} > 0$ : Strain Hardening	$\frac{\partial F}{\partial \varepsilon_{ij}} d\varepsilon_{ij} > 0$ : Strain Hardening
$\frac{\partial f}{\partial \sigma_{ij}} d\sigma_{ij} < 0$ : Strain Softening	$\frac{\partial F}{\partial \varepsilon_{ij}} d\varepsilon_{ij} > 0$ : Strain Softening
$\frac{\partial f}{\partial \sigma_{ij}} d\sigma_{ij} = 0$ : Perfect Plasticity	$\frac{\partial F}{\partial \varepsilon_{ij}} d\varepsilon_{ij} > 0$ : Perfect Plasticity
(c) Neutral Condition	
$\frac{\partial f}{\partial \sigma_{ij}} d\sigma_{ij} = 0$	$\frac{\partial F}{\partial \varepsilon_{ij}} d\varepsilon_{ij} = 0$
(d) Unloading Condition	
$\frac{\partial f}{\partial \sigma_{ij}} d\sigma_{ij} < 0$	$\frac{\partial F}{\partial \varepsilon_{ij}} d\varepsilon_{ij} < 0$
(e) Flow Rule	
<p>Drucker's Postulate</p> $d\varepsilon_{ij}^p = d\lambda \frac{\partial f}{\partial \sigma_{ij}}$  <p style="text-align: center;"><math>f = 0</math></p>	<p>Il'yushin's Postulate</p> $d\sigma_{ij}^p = d\lambda \frac{\partial F}{\partial \varepsilon_{ij}}$  <p style="text-align: center;"><math>F = 0</math></p>
(f) Stress-Strain Relation	
Use Consistency Condition	Use Consistency Condition

In the present research, a loading function  $F$  in the strain space is defined through the following transformation of Eq.(15) by Eq.(3).

The hydrostatic pressure  $p$  and the deviatoric stresses  $s_{ij}$  are written in terms of the strain as

$$p = K (\varepsilon_{ii} - \varepsilon_{ii}^p) \quad (16)$$

$$s_{ij} = 2 \mu (e_{ij} - e_{ij}^p), \quad (17)$$

where  $K$ ,  $\mu$ ,  $e_{ij}$ , and  $e_{ij}^p$  = the bulk modulus, the shear modulus, the deviatoric strain tensor, and the plastic deviatoric strain tensor, respectively.

Thus, the stress invariants  $I_1$ ,  $J_2$ , and  $J_3$  are written as

$$I_1 = 3 p = 3K (\varepsilon_{ii} - \varepsilon_{ii}^p) \quad (18.a)$$

$$J_2 = \frac{1}{2} s_{ij}s_{ij} = 2 \mu^2 (e_{ij} - e_{ij}^p)(e_{ij} - e_{ij}^p) \quad (18.b)$$

$$J_3 = \frac{1}{3} s_{ij}s_{jk}s_{ki} = \frac{8}{3} \mu^3 (e_{ij} - e_{ij}^p)(e_{jk} - e_{jk}^p)(e_{ki} - e_{ki}^p). \quad (18.c)$$

Further, introducing the following strain invariants  $\bar{I}_1$ ,  $\bar{J}_2$ , and  $\bar{J}_3$  defined by

$$\bar{I}_1 = \varepsilon_{ii} - \varepsilon_{ii}^p \quad (19.a)$$

$$\bar{J}_2 = \frac{1}{2} (e_{ij} - e_{ij}^p)(e_{ij} - e_{ij}^p) \quad (19.b)$$

$$\bar{J}_3 = \frac{1}{3} (e_{ij} - e_{ij}^p)(e_{jk} - e_{jk}^p)(e_{ki} - e_{ki}^p), \quad (19.c)$$

the stress invariants of Eq.(18) can be rewritten as

$$I_1 = \bar{A} \bar{I}_1 \quad (20.a)$$

$$J_2 = \bar{B} \bar{J}_2 \quad (20.b)$$

$$J_3 = \bar{C} \bar{J}_3, \quad (20.c)$$

where  $\bar{A} = 3K$ ,  $\bar{B} = 4 \mu^2$ ,  $\bar{C} = 8 \mu^3$ .

Substitution of Eqs.(20) into Eq.(15) leads to the Lade type of loading surface  $F$

$$F = (\bar{A} \bar{I}_1 + a)^3 - [27 + f_p \left( \frac{P a}{\bar{A} \bar{I}_1 + a} \right)^m] \times \left[ \frac{1}{27} (\bar{A} \bar{I}_1 + a)^3 - \frac{1}{3} (\bar{A} \bar{I}_1 + a) \bar{B} \bar{J}_2 + \bar{C} \bar{J}_3 \right] = 0. \quad (21)$$

**Figure 1** shows a schematic view of Eq.(21) with the different values of loading parameters  $f_p$  in the principal elastic-strain space.

### 3.2 Plastic Potential Function $G$

It is found that, in the present research, the plastic potential surface determined from the procedure by Lade [23] does not give a good prediction of the plastic volumetric strain compared with the experimental data. For example, for the case that a dilatancy is expected to occur, the model may predict a compaction. Thus, a new procedure to define a plastic potential function  $G$  has

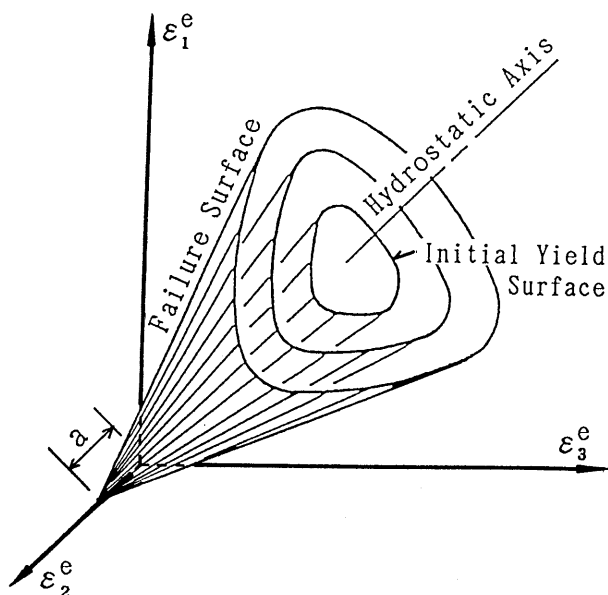


Fig.1 Lade Loading Surface in Strain Space

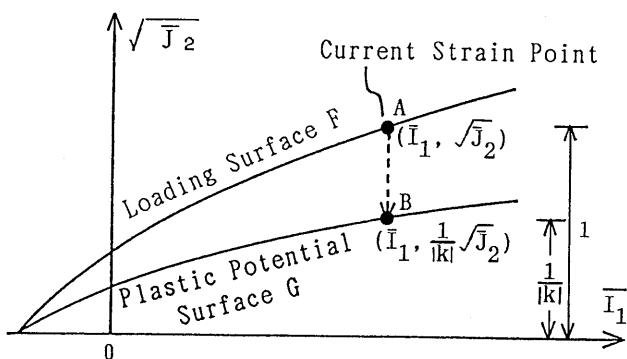


Fig.2 Definition of Plastic Potential Surface in Strain Space

been proposed in the following manner: Assuming that the current strain state is at point A( $\bar{I}_1, \sqrt{J_2}$ ) on the current loading surface F, as shown in Fig.2, the plastic potential surface G is defined so that it has the same apex as that of the loading surface F and passes through a specific point B( $\bar{I}_1, \sqrt{J_2}/|k|$ ) where k is a variable. As a special case, when  $1/k$  is 1, the plastic potential function G becomes identical to the loading function F, while it becomes the von Mises type when  $1/k$  is zero. The normal tensor  $\partial G / \partial \epsilon_{ij}$  calculated at this specific point B is directly used in Eq.(14) for the case of a positive value k, while for a negative value k, the tensor with the same deviatoric components but a negative volumetric component to that of  $\partial G / \partial \epsilon_{ij}$  is used in Eq.(14).



#### 4. MODEL CALIBRATION

In the following, the strain-space-based plasticity model developed in the preceding section is calibrated by using the triaxial compression test data to simulate the hardening and softening behavior of concrete.

##### 4.1 Experimental Data

The experimental data used for model calibration are obtained from the triaxial compression tests on cubic plain concrete specimen ( $10\text{cm} \times 10\text{cm} \times 10\text{cm}$ ) with the water/cement ratios (W/C ratios) of 0.45, 0.55, and 0.7, under the different confining pressures  $\sigma_c = 0 \text{ kgf/cm}^2$  (0 kPa),  $1 \text{ kgf/cm}^2$  (98 kPa),  $3 \text{ kgf/cm}^2$  (294 kPa),  $6 \text{ kgf/cm}^2$  (588 kPa), and  $12 \text{ kgf/cm}^2$  (1176 kPa) [8]. Specimens were loaded axially under the constant strain rate of about  $2 \times 10^{-3} \text{ min.}^{-1}$ , by using a high-rigidity compression testing machine. The friction at the interface between specimen and loading plate was reduced by placing the friction-reducing pads that consist of two polypropylene sheets with silicon grease between them. Further information on testing conditions and procedures is given in the earlier papers [7][8].

Note that the experimental data under a confining pressure  $\sigma_c = 12 \text{ kgf/cm}^2$  (1176 kPa) are available only for the concrete specimen with W/C ratio = 0.55. These experimental data are shown later with several symbols in Figs.13 through 15.

##### 4.2 Determination of Material Parameters

The following material parameters are required in the proposed model.

###### (A) Elastic Constants

Since concrete is here assumed to be linearly isotropic in the elastic range, only two material constants, such as the bulk modulus  $K$  and the shear modulus  $\mu$ , are determined by using the initial portion of stress-strain curves from uniaxial compression tests (confining pressure  $\sigma_c = 0 \text{ kgf/cm}^2 = 0 \text{ kPa}$ ) for the different W/C ratios. These values are presented in Table 2.

Table 2. Elastic Moduli

Water/Cement Ratio (W/C)	Bulk Modulus $K$ ( $\text{kgf/cm}^2$ )	Shear Modulus $\mu$ ( $\text{kgf/cm}^2$ )
0.45	166,667	125,000
0.55	150,000	112,500
0.70	133,333	100,000

Note:  $1 \text{ kgf/cm}^2 = 98 \text{ kPa}$

###### (B) Parameters for Failure Surface

The parameters in Eq.(21) at the failure state are  $\eta_1$ ,  $m$ , and  $a$ . As shown in Fig.3, the failure states corresponding to all 13 sets of experimental data

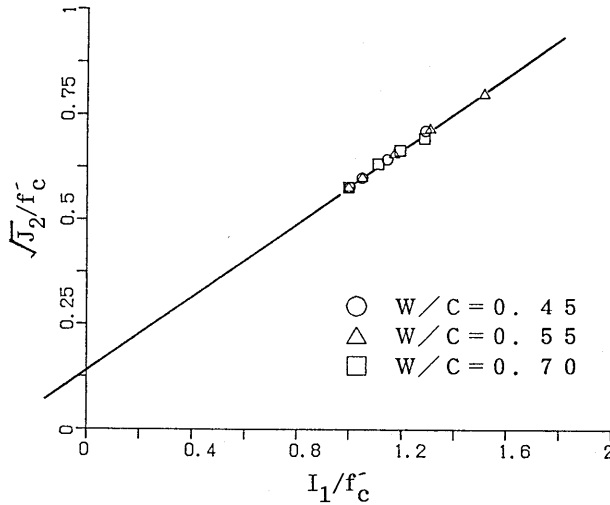


Fig.3 Failure Points in Nondimensional Stress Invariant Space

are plotted in the nondimensional stress invariant space ( $I_1/f'_c$ ,  $\sqrt{J_2}/f'_c$ ) where  $f'_c$  is the uniaxial compressive strength, that is, 338 (33.1), 273 (26.8), and 216 kgf/cm<sup>2</sup> (21.2 MPa) for the W/C ratio of 0.45, 0.55, and 0.7, respectively. Three parameters are evaluated as  $\eta_1 = 165$  (maximum value of  $f_p$ ),  $m = 0$ , and  $a = 0.31 f'_c$  in tension side. For the case of parameter  $m = 0$ , a meridian of failure surface becomes a straight line and overestimates the  $a$ -value that is usually on the order of  $(0.1 - 0.15) f'_c$ .

Since the concrete is known to exhibit linearly elastic behavior up to about 30 % of failure strength [14], the initial loading surface is located at a level of  $f_p = 26$ .

### (C) Loading Parameter

The loading parameter  $f_p$  is defined as a function of plastic work  $W_p$  ( $= \int \sigma_{ij} d\epsilon_{ij}$ ), that is,

$$f_p = \alpha \exp(-\beta W_p) \left(\frac{W_p}{P_a}\right)^{\frac{1}{\gamma}}, \quad (22)$$

where  $P_a$  = an atmospheric pressure; and  $\alpha$ ,  $\beta$ , and  $\gamma$  = parameters. The parameters  $\alpha$  and  $\beta$  are defined as functions of the parameter  $\gamma$  and the plastic work  $W_{ppeak}$  corresponding to the peak value  $\eta_1$  of parameter  $f_p$ . These mathematical expressions are given as [23]

$$\alpha = \eta_1 \left(\frac{e P_a}{W_{ppeak}}\right)^{\frac{1}{\gamma}} \quad (23)$$

$$\beta = \frac{1}{\gamma W_{ppeak}}, \quad (24)$$

where  $e$  = the natural logarithmic base.

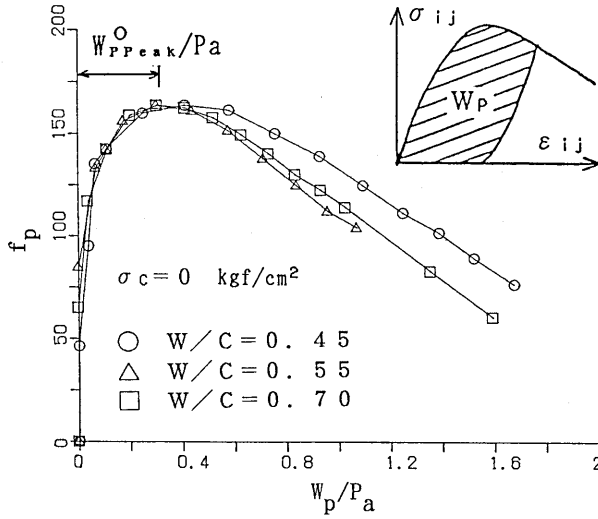


Fig.4  $f_p - W_p/P_a$  Relation ( $\sigma_c = 0 \text{ kgf/cm}^2$ ;  $1 \text{ kgf/cm}^2 = 98 \text{ kPa}$ )

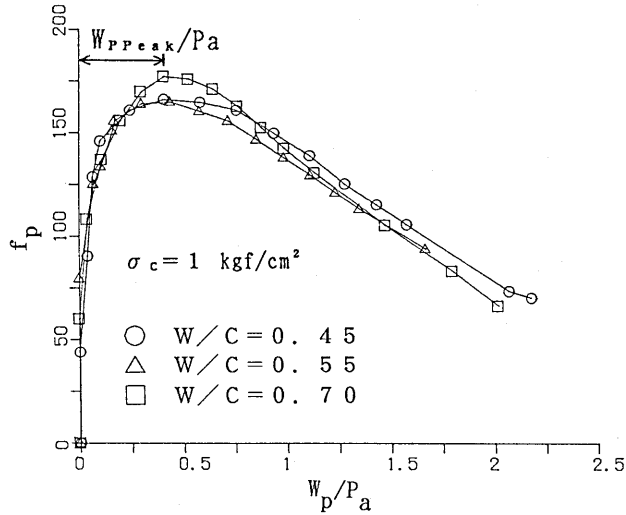


Fig.5  $f_p - W_p/P_a$  Relation ( $\sigma_c = 1 \text{ kgf/cm}^2$ ;  $1 \text{ kgf/cm}^2 = 98 \text{ kPa}$ )

The  $f_p - W_p/P_a$  relations calculated from the experimental data are shown in Figs.4, through 7 for each confining pressure 0, 1 (98kPa), 3 (294 kPa), and 6  $\text{kgf/cm}^2$  (588 kPa). It can be understood from these figures that there seems to be a similar relation between  $f_p$  and  $W_p/P_a$  under the same confining pressure, irrespective of the different  $W/C$  ratios.

Utilizing the averaged value  $W_{p\text{peak}}$  of plastic works corresponding to the peak values of  $f_p$  in the  $f_p - W_p/P_a$  relations under the same confining pressure (in Figs.4 through 7), the correlation between  $(W_{p\text{peak}} - W_{p\text{peak}}^0)/P_a$  and  $\sigma_c/P_a$  is checked in the  $\ln - \ln$  diagram (Fig.8). Here,  $W_{p\text{peak}}^0$  is the averaged plastic work ( $0.345 \text{ kgf/cm}^2 = 33.8 \text{ kPa}$ ) corresponding to the peak value of  $f_p$  under confining pressure  $\sigma_c = 0 \text{ kgf/cm}^2$ . A strong linear correlation can be seen in Fig.8 and, thus, written mathematically as

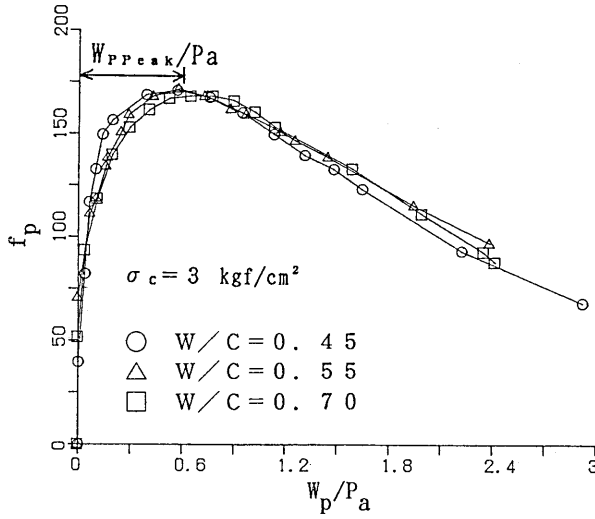


Fig.6  $f_p - W_p/P_a$  Relation ( $\sigma_c = 3 \text{ kgf/cm}^2$ ;  $1 \text{ kgf/cm}^2 = 98 \text{ kPa}$ )

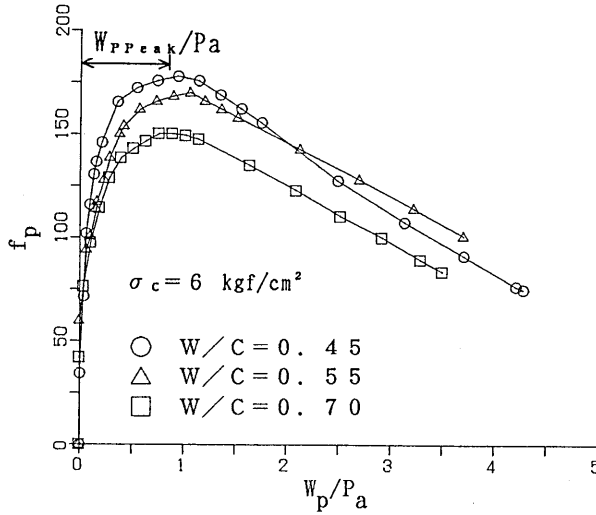


Fig.7  $f_p - W_p/P_a$  Relation ( $\sigma_c = 6 \text{ kgf/cm}^2$ ;  $1 \text{ kgf/cm}^2 = 98 \text{ kPa}$ )

$$W_{p\text{peak}} = P \left( \frac{\sigma_c}{P_a} \right)^{\varrho} P_a + W_{p\text{peak}}^0 \quad (25)$$

where  $P$  and  $\varrho$  = constants. Using the method of least squares,  $P$  and  $\varrho$  are estimated as 0.099 and 0.867, respectively.

On the other hand, the values of parameter  $\gamma$  for confining pressures  $\sigma_c = 0, 1 (98), 3 (294), 6 (588), \text{ and } 12 \text{ kgf/cm}^2 (1176 \text{ kPa})$  are determined by a curve-fitting method so that the curve calculated by Eq.(22) results in a good agreement with the  $f_p - W_p/P_a$  relations in Figs.4 through 7. The variation of  $\gamma$  values is shown in Fig.9 where a strong linear correlation between  $\gamma$  and  $\sigma_c$  can be seen. It can be written mathematically as

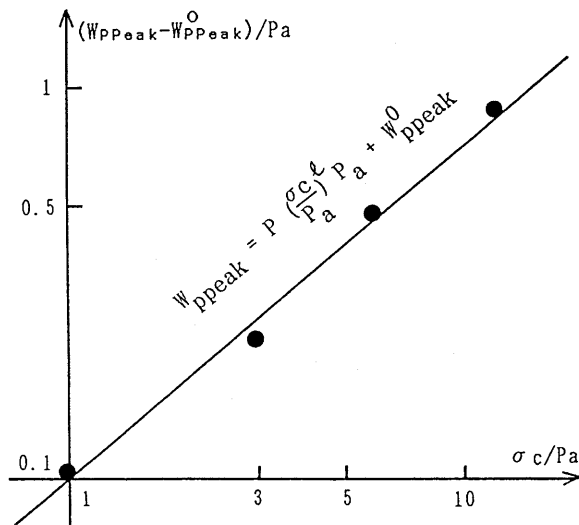


Fig.8  $\ln((W_{peak} - W_{peak}^0)/P_a) - \ln(\sigma_c/P_a)$  Relation

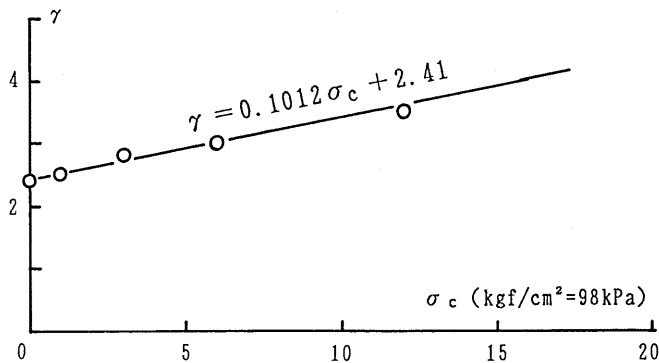


Fig.9 Variation of Parameter  $\gamma$

Table 3. Model Parameters

Constant	Units	Value
$\eta_1$	—	165
$m$	—	0.
$a$	—	0.31 $f'_c$
$P$	—	0.099
$q$	—	0.867
$W_{peak}^0$	kgf/cm <sup>2</sup>	0.345
$\gamma_1$	cm <sup>2</sup> /kgf	0.1012
$\gamma_2$	—	2.41

Note:  $f'_c = 338 \text{ kgf/cm}^2$  for  $W/C = 0.45$ ;  $273 \text{ kgf/cm}^2$  for  $W/C = 0.55$   
 $216 \text{ kgf/cm}^2$  for  $W/C = 0.70$ ;  $1 \text{ kgf/cm}^2 = 98 \text{ kPa}$

$$\gamma = \gamma_1 \sigma_c + \gamma_2, \quad (26)$$

where  $\gamma_1 = 0.1012 \text{ cm}^2/\text{kgf}$  ( $1.033 \times 10^{-3} \text{ kPa}^{-1}$ ), and  $\gamma_2 = 2.41$ .

The material parameters, such as for failure and loading, determined in the present study are summarized in **Table 3**.

#### (D) Parameter k in Plastic Potential Function G

The value k to define the plastic potential function G is calculated by using the plastic volumetric strain increment and square root of the second

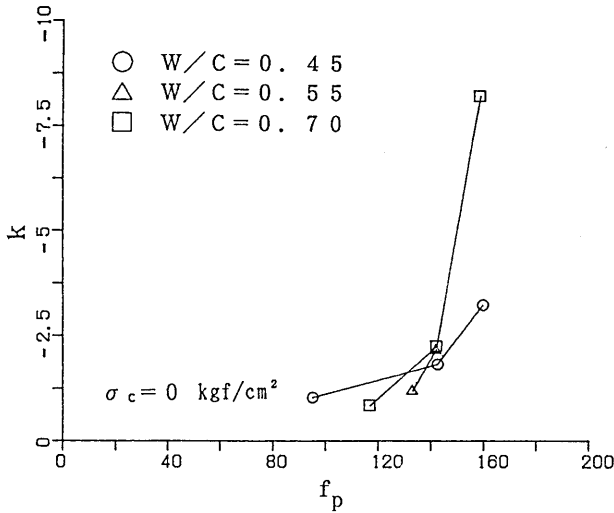


Fig.10 Variation of k-Value in Hardening Region

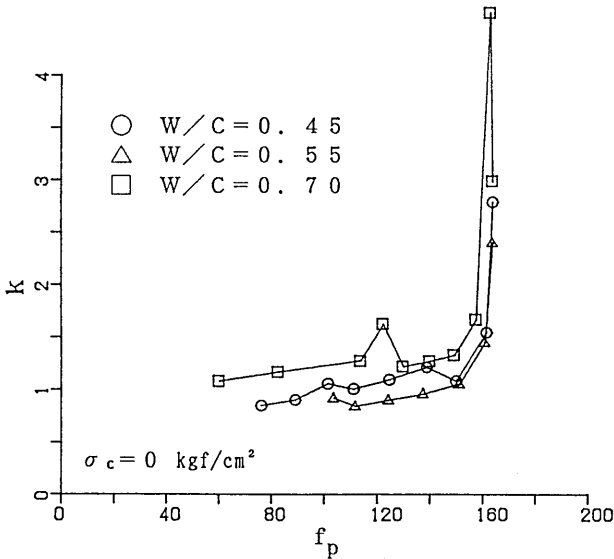
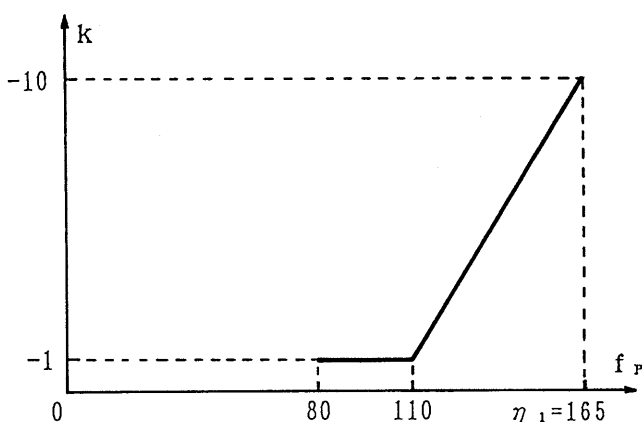


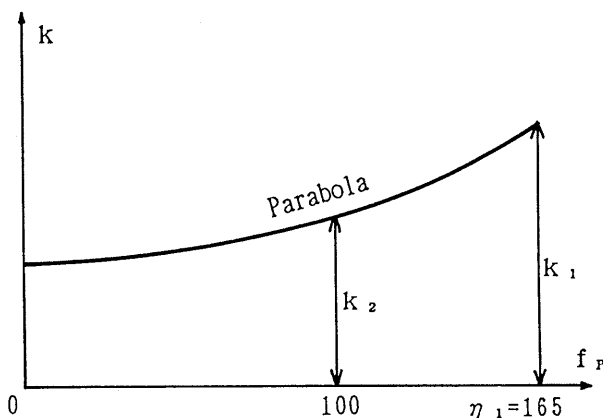
Fig.11 Variation of k-Value in Softening Region

invariant of incremental plastic strain tensor that are obtained from experimental data. The variations of  $k$  values before and after the peak stress ( $\eta_1 = 165$ ) are examined for each confining pressure, 0, 1 (98), 3 (294), 6 (588), and 12 kgf/cm<sup>2</sup> (1176 kPa). As an example, the variations of  $k$  values before and after the peak stress are shown in Figs.10 and 11, respectively, for a confining pressure  $\sigma_c = 0$  kgf/cm<sup>2</sup>.

From these figures, the following characteristics can be concluded: In the hardening region (before the peak stress), the parameter  $k$  has a negative value of approximately -1 around  $f_p = 90$ , and gradually increases in magnitude up to the value more than -10, as the loading parameter  $f_p$  approaches the peak value ( $f_p = 165$ ). On the other hand, in the softening region (after the peak stress), as the loading parameter  $f_p$  decreases from the peak value, it shows a mild



(a) Hardening Region



(b) Softening Region

Fig.12 Idealized Variation of  $k$ -Value

reduction between the values of 2 and 1, after a sudden reduction of positive k-value at the peak stress. A negative value before the peak stress, a large negative/positive value in the vicinity of peak stress, and a positive value after peak stress are related to plastic compaction, little plastic volumetric change, and dilatancy, respectively.

In the present model development, the variations of parameter k in the hardening and softening region are assumed from the experimental data, as shown in Fig.12, and incorporated into the model simulation. The values of  $k_1$  (the value of parameter k at  $f_p = \eta_1$ ) and  $k_2$  (the value of parameter k at  $f_p = 100$ ) in the softening region are presented in Table 4, for all 13 sets of experimental data.

Table 4. The Values of Parameter k

Water/ Cement Ratio	k values under $\sigma_c = 0$ kgf/cm <sup>2</sup>		k values under $\sigma_c = 1$ kgf/cm <sup>2</sup>		k values under $\sigma_c = 3$ kgf/cm <sup>2</sup>		k values under $\sigma_c = 6$ kgf/cm <sup>2</sup>		k values under $\sigma_c = 12$ kgf/cm <sup>2</sup>	
	$k_1$	$k_2$	$k_1$	$k_2$	$k_1$	$k_2$	$k_1$	$k_2$	$k_1$	$k_2$
W/C										
0.45	1.6	1.1	2.0	1.2	2.0	1.5	2.2	1.8	-	-
0.55	1.2	1.1	1.7	1.1	2.0	1.3	2.0	1.6	3.5	2.0
0.70	2.0	1.4	2.0	1.6	2.1	1.6	3.0	2.0	-	-

Note: 1 kgf/cm<sup>2</sup> = 98 kPa

## 5. MODEL SIMULATION AND EVALUATION

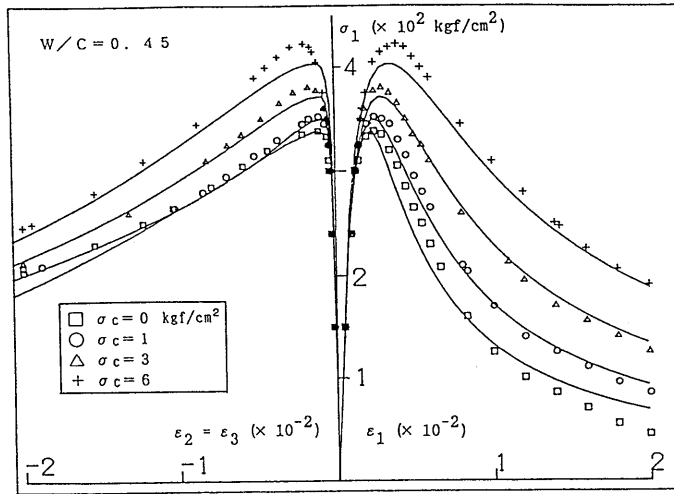
Using the model parameters determined in the previous section, the model simulation has been performed for the experimental data, to assess a representation capacity of the model. The axial strain  $\varepsilon_1$ /lateral strain  $\varepsilon_2 = \varepsilon_3$  - axial stress  $\sigma_1$  relation and the axial strain  $\varepsilon_1$  - volumetric strain  $\varepsilon_v$  relation are shown in Figs.13 through 15, where the solid lines and symbols represent the model simulations and experimental data, respectively. In these figures, the compressive stress and strain are taken as positive. The model can simulate well not only the axial strain but also the lateral strains. This means that the plastic potential function G has been correctly assumed in the modeling.

## 6. CONCLUDING REMARKS

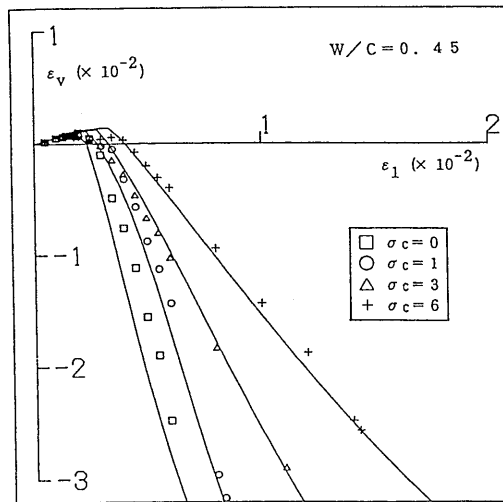
In this paper, a strain-space-based plasticity model has been proposed to represent the softening as well as hardening behavior of concrete materials under low lateral confining pressure. Unlike the stress-space plasticity theory based on the Drucker's postulate, the strain-space plasticity theory based on the Il'yushin's postulate can give a clear definition of loading (hardening, softening, and perfect plasticity), neutral loading, and unloading.

The general strain-space formulation, which is of great advantage in representing the softening behavior of concrete and in application to the finite





(a) Axial Stress - Axial Strain - Lateral Strain Relation



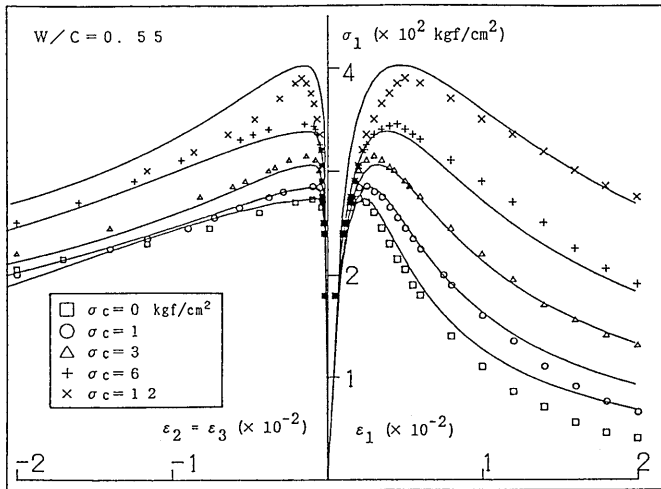
(b) Volumetric Strain - Axial Strain Relation

Fig.13 Model Simulation ( $W/C = 0.45$ ;  $1\text{kgf/cm}^2 = 98\text{ kPa}$ )

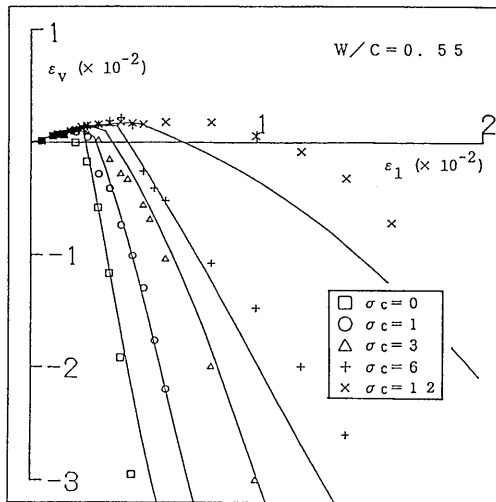
element elastic-plastic analysis of RC structures, has been presented in some detail within the framework of the associated and nonassociated flow rule, by introducing the loading function  $F$  and the plastic potential function  $G$ , which are functions of the strain, plastic strain, and loading parameter.

The incremental stress-strain relations have been given in a tensorial form. Use of the Lade type of loading function and newly defined plastic potential function has been made in the incremental stress-strain equation.

The proposed model requires only a few parameters. These are elastic modu-



(a) Axial Stress - Axial Strain - Lateral Strain Relation



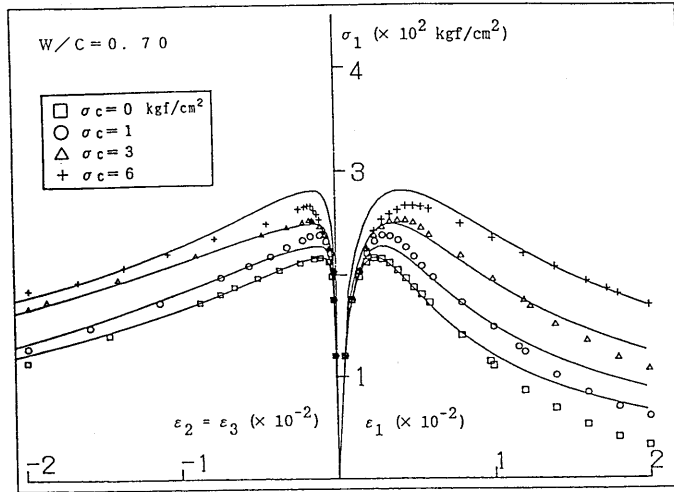
(b) Volumetric Strain - Axial Strain Relation

Fig.14 Model Simulation ( $W/C = 0.55$ ;  $1\text{kgf/cm}^2 = 98\text{ kPa}$ )

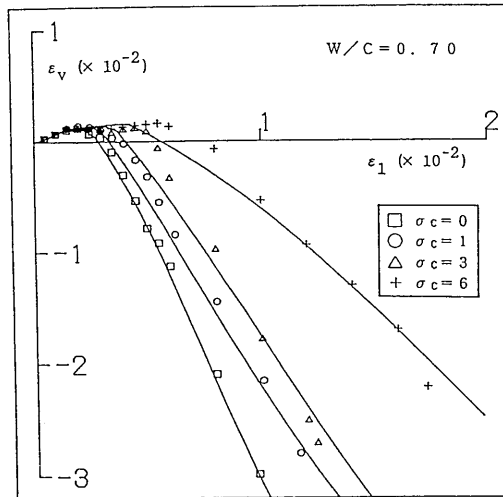
li  $K$  and  $\mu$ ; failure surface parameters,  $\eta$ ,  $m$ , and  $a$ ; loading parameter  $f_p$ ; and parameter  $k$  related to the plastic potential function  $G$ .

Using the triaxial compression test data available, the model parameters have been determined with relative ease, and then model simulation has been performed to demonstrate the representation capability of the model.

Although the capability of the proposed model was demonstrated by being applied back to the experimental data that are used to determine the model parameters, it should be noted that unified parameter functions such as  $W_{\text{peak}}$



(a) Axial Stress - Axial Strain - Lateral Strain Relation



(b) Volumetric Strain - Axial Strain Relation

Fig.15 Model Simulation ( $W/C = 0.70$ ;  $1 \text{ kgf/cm}^2 = 98 \text{ kPa}$ )

and  $\gamma$  given by Eqs.(25) and (26) are used for all back-predictions of three types of concretes. Even though an  $f_p - W_p$  relation in Eq.(22) was exactly fitted with the experimental data, the relations shown in Figs.13 through 15 could not be obtained unless a plastic potential function was moderately defined.

It has been confirmed that the proposed model can sufficiently predict the softening as well as hardening behavior of concrete materials under low lateral confining pressure. The two-dimensional or three-dimensional softening behavior of concrete under varying confining pressures, nonproportional loadings and unloadings are now undertaken as a further research work.

## ACKNOWLEDGMENTS

This work is partially supported by the Grant from the Ministry of Education, Science and Culture of the Japanese Government (Grant No. 63550409). Professor Yasuo Tanigawa of Nagoya University is also acknowledged for his fruitful discussion and support through the work.

## APPENDIX I. CREDIT LINE

This paper is rearranged from the following papers:

- (1) Mizuno, E., and Hatanaka, S., "Strain space plasticity modeling for compressive softening behavior of concrete materials." Concrete Research and Technology, JCI, 2(2), pp.85-95, 1991
- (2) Mizuno, E., and Hatanaka, S., "Compressive softening model for concrete." J. Engrg. Mech., ASCE, 118(8), pp.1546-1563, 1992 (the material of present paper is reproduced by permission of ASCE)

## APPENDIX II. REFERENCES

- [1] Bažant, Z.P., and Kim, S.S., "Plastic-fracturing theory for concrete." ASCE National Convention, 1978
- [2] Yang, B.L., Dafalias, Y.F., and Herrmann, L.R., "A bounding surface plasticity model for concrete." J. Engrg. Mech., ASCE, 111(3), 1985
- [3] Han, D.J., and Chen, W.F., "Strain-space plasticity formulation for hardening-softening materials with elastoplastic coupling." Int. J. Solids Structures, 22(8), 1986
- [4] Frantziskonis, G., and Desai, C.S., "Constitutive model with strain softening." Int. J. Solids Structures, 23(6), 1987
- [5] Wu, Z., and Tanabe, T., "A hardening/softening model of concrete subjected to compressive loading," Jour. of Struct. Engrg., JSCE, 36B, 1990
- [6] Kosaka, Y., Tanigawa, Y., and Hatanaka, S., "Inelastic deformational behavior of axially loaded concrete under low lateral confining stresses." Trans. of Japan Concrete Inst., 6, 1984
- [7] Kosaka, Y., Tanigawa, Y., and Hatanaka, S., "Lateral confining stresses due to steel fibers in concrete under compression." The International Jour. of Cement Composites, 7(2), 1985
- [8] Hatanaka, S., Kosaka, Y., and Tanigawa, Y., "Plastic deformational behavior of axially loaded concrete under low lateral pressure - an evaluation method for compressive toughness of laterally confined concretes - (Part I)." J. Structural and Construction Engineering, (Trans. of AIJ), 377, 1987
- [9] Kotsovos, M.D., and Newman, J.B., "Mathematical description of deformational behavior of concrete under generalized stress beyond ultimate strength," Jour. of ACI, 77(5), 1980
- [10] Ahmad, S.H., and Shah, S.P., "Complete triaxial stress-strain curves for concrete," J. Struct., ASCE, 108(4), 1982
- [11] Willam, K., Hurlbut, B., and Sture, S., "Experimental constitutive and computational aspects of concrete failure," Seminar on FEM Anal. of RC St., Tokyo, JCI, 1, 1985
- [12] Van Mier, J.G.M., "Complete stress-strain behavior and damaging status of concrete under multiaxial conditions," RILEM-CEB-CNRS, Int. Conf. on Concrete under Multiaxial Conditions, Vol.1, Presses de l'Université Paul Sabatier, Toulouse, France, 1984
- [13] Drucker, D.C., "Some implications of work hardening and ideal plasticity." Q. Appl. Math., 7(4), 1950
- [14] Chen, W.F., Plasticity in reinforced concrete, McGraw-Hill, New York, N.Y., 1982

- [15] Chen, W.F., and Han, D.J., Plasticity for structural engineers. Springer-Verlag. 1988
- [16] Chen, W.F., and Mizuno, E., Nonlinear analysis in soil mechanics - theory and implementation -, Elsevier, Amsterdam, 1990
- [17] Il'yushin, A.A., "On the postulate of plasticity." Prikl. Mat. Mekh., 25, 1961
- [18] Naghdi, P.M., and Trapp, J.A., "The significance of formulating plasticity theory with reference to loading surfaces in strain space." Int. J. Engng. Sci., 13, 1975
- [19] Casey, J., and Naghdi, P.M., "On the characterization of strain-hardening in plasticity." J. Appl. Mech., ASME, 48, 1981
- [20] Casey, J., and Naghdi, P.M., "On the nonequivalence of the stress space and strain space formulations of plasticity theory." J. Appl. Mech., ASME, 50, 1983
- [21] Yoder, P.J., and Iwan, W.D., "On the formulation of strain-space plasticity with multiple loading surfaces." J. Appl. Mech., ASME, 48, 1981
- [22] Kioussis, P.D., "Strain space approach for softening plasticity." J. Engrg. Mech., ASCE, 113(2), 1987
- [23] Lade, P.V., "Elasto-plastic stress-strain theory for cohesionless soil with curved yield surfaces." Int. J. Solids Structures, 13, 1977
- [24] Lade, P.V., "Three-parameter failure criterion for concrete." J. Engrg. Mech., ASCE, 108(5), 1982